Linear Instability of Planar Shear Banded Flow

S. M. Fielding*
Polymer IRC and School of Physics & Astronomy, University of Leeds, Leeds LS2 9JT, United Kingdom
(Received 21 January 2005; published 20 September 2005)

We study the linear stability of planar shear banded flow with respect to perturbations with wave vector in the plane of the banding interface, within the nonlocal Johnson-Segalman model. We find that perturbations grow in time, over a range of wave vectors, rendering the interface linearly unstable. Results for the unstable eigenfunction are used to discuss the nature of the instability. We also comment on the stability of phase separated domains to shear flow in model H.

DOI: 10.1103/PhysRevLett.95.134501 PACS numbers: 47.50.+d, 47.55.Kf, 61.25.Hq, 83.60.Wc

Complex fluids such as wormlike [1] and onion [2] surfactants, polymer solutions [3], and soft glasses [4] commonly show flow instabilities and flow-induced transitions to shear banded states. This behavior is captured by several notable rheological models [5] in which the underlying constitutive curve of shear stress vs shear rate, $T_{xy}(\dot{\gamma})$, is nonmonotonic (Fig. 1), allowing bands of differing shear rate to coexist at common shear stress, Fig. 2. To ensure unique, history independent stress selection ($T_{xy} = T_b$ in Fig. 1), any constitutive model must include spatially nonlocal terms to allow a smooth interfacial profile between the bands, Fig. 2 [6]. While this scenario is widely accepted, most existing studies consider only one spatial dimension ($D = 1$) [6,7], normal to the interface (the flow-gradient direction, y). The stability of these banded states in $D > 1$ dimensions has been implicitly assumed, but is, in fact, an open question.

In this Letter, therefore, we study the linear stability of 1D shear banded states to perturbations with wave vectors in the interfacial plane $(x, z) =$ (flow, vorticity). We work within the nonlocal "diffusive" Johnson-Segalman (DJS) model [8,9], which is often taken as a paradigm of shear banding systems. We show that perturbations typically grow in time, rendering the 1D banded profile unstable. This finding opens the way to nontrivial interfacial dynamics and could help to understand data revealing erratic fluctuations of shear banded flows [10], forming a timely counterpart to new experimental techniques probing interface dynamics [11]. It is also relevant industrially to processing instability and oil extraction. The stability of (unphysical) *sharp* interfaces in a spatially *local* model was studied in Ref. [12]; we contrast that study with ours below.

The model is defined as follows. The momentum balance equation for a polymeric fluid of density ρ is

$$\rho(\partial_t + \mathbf{V}\cdot\nabla)\mathbf{V} = \nabla\cdot(\mathbf{\Sigma} + \eta\nabla\mathbf{V} - P\mathbf{I}), \qquad (1)$$

where $\mathbf{V}(\mathbf{R})$ is the velocity field, η the solvent viscosity (assumed Newtonian), and $\mathbf{\Sigma}(\mathbf{R})$ the viscoelastic stress carried by the polymeric molecules. For homogeneous planar shear, $\mathbf{V} = y\dot{\gamma}\hat{\mathbf{x}}$, the total shear stress $T_{xy} = \Sigma_{xy}(\dot{\gamma}) + \eta\dot{\gamma}$. The pressure P is set by incompressibility,

$$\nabla\cdot\mathbf{V} = 0. \qquad (2)$$

The polymeric stress is taken to obey DJS dynamics [8,9]

$$\overset{\diamond}{\mathbf{\Sigma}} = 2G\mathbf{D} - \frac{\mathbf{\Sigma}}{\tau} + \frac{l^2}{\tau}\nabla^2\mathbf{\Sigma} \qquad (3)$$

with time derivative

$$\overset{\diamond}{\mathbf{\Sigma}} = (\partial_t + \mathbf{V}\cdot\nabla)\mathbf{\Sigma} - a(\mathbf{D}\cdot\mathbf{\Sigma} + \mathbf{\Sigma}\cdot\mathbf{D}) - (\mathbf{\Sigma}\cdot\mathbf{\Omega} - \mathbf{\Omega}\cdot\mathbf{\Sigma})$$

in which $\mathbf{D}$ and $\mathbf{\Omega}$ are the symmetric and antisymmetric parts of the velocity gradient tensor, $(\nabla\mathbf{V})_{\alpha\beta} \equiv \partial_\alpha v_\beta$. For $a = 1$ and $l = 0$ this model reduces to the Oldroyd B model, which can be motivated by considering an ensemble of beads paired into dumbbells by Hookean springs (simplified polymer chains). Stress is generated as the flow affinely deforms dumbbells with plateau modulus G, and relaxed on the time scale τ for the springs to regain their equilibrium length. To capture shear thinning, the DJS model invokes a "slip parameter" a with $|a| < 1$ to allow nonaffine dumbbell deformation [8]. The constitutive curve $T_{xy}(\dot{\gamma})$ is then capable of nonmonotonicity, Fig. 1. The nonlocal diffusive term accounts for spatial gradients across the banding interface on a length scale l. It arises naturally in models of liquid crystals, and diffusion of strained polymer molecules [13]. Within this model we study shear between parallel plates at $y = 0, L$. We set

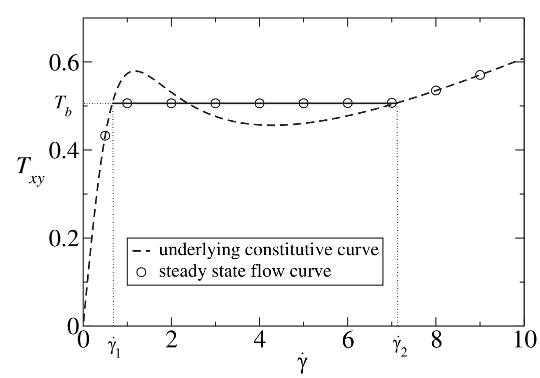

FIG. 1. Underlying constitutive curve; steady state flow curve. $a = 0.3$, $\eta = 0.05$. Banding occurs on the plateau.

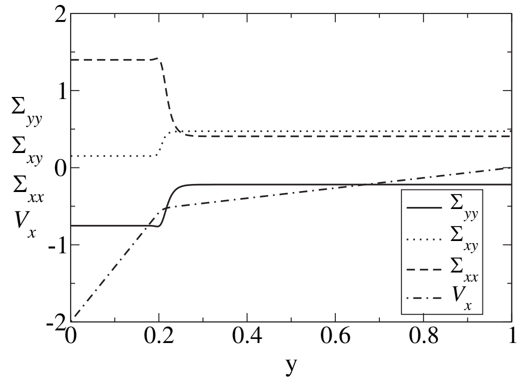

FIG. 2. A 1D banded profile, with spatial gradients restricted to the flow-gradient direction, y. $\bar{\dot\gamma} = 2.0$, towards the left of the plateau in Fig. 1. $l = 0.01$, $N_{\mathrm{base}} = 800$. Note the total shear stress T_{xy} is uniform across the cell.

$G = 1$, $\tau = 1$, and $L = 1$, and use boundary conditions at $y = 0, 1$ of $\partial_y \Sigma_{\alpha\beta} = 0 \;\forall\; \alpha, \beta$, with no slip and no penetration for the velocity.

For an imposed shear rate $\bar{\dot\gamma}$ in the region of decreasing stress, $dT_{xy}/d\dot\gamma < 0$, homogeneous flow is unstable [14]. A 1D analysis in the flow-gradient dimension then predicts separation into two bands of shear rates $\dot\gamma_1$, $\dot\gamma_2$ and shear stress, T_{b}, separated by an interface of width $O(l)$. As the applied shear rate $\bar{\dot\gamma}$ increases across the banding regime, the width fraction of the bands adjusts to maintain the constraint $\int dy \dot\gamma(y) = \bar{\dot\gamma}$, while $\dot\gamma_1$, $\dot\gamma_2$, and T_{b} stay constant, giving a plateau in the steady state flow curve (Fig. 1). We verified this scenario by numerically evolving Eqs. (1)–(3), allowing spatial variations only in the flow-gradient direction y. We used a Crank Nicholson algorithm [15] with a finite difference scheme on a uniform mesh of "full" points $y_0, y_1, \ldots, y_{N_{\mathrm{base}}}$ for $\mathbf{\Sigma}$ and staggered "half" points $y_{1/2}, y_{3/2}, \ldots, y_{N_{\mathrm{base}}-(1/2)}$ for $\mathbf{V}$. We evolved with time step Dt for a time $t_{\max}$ to steady state, checking for convergence to $N_{\mathrm{base}} \to \infty$, $Dt \to 0$, $t_{\max} \to \infty$.

The flow curve is shown in Fig. 1, and a banded profile in Fig. 2. The smooth variation of $\mathbf{\Sigma}$ across the interface, of width $O(l)$, results from the diffusive term in Eq. (3). By contrast, in local models ($l = 0$) the interface is an unphysical sharp discontinuity. The local case is also pathological in the sense that this sharply banded state is not uniquely selected, but chosen by flow history from a continuum of candidates [6,9]. The stability of these sharp interfaces, sampled from this continuum, was studied previously. Renardy [16] found instability in the limit of a thin high shear band in the local JS model. McLeish [12] studied the Poiseuille flow of a modified local Doi-Edwards model and found a long wavelength ($q_x \to 0$) instability due to the jump in normal stresses across the interface. This was also discussed in Ref. [17].

Here we study the *nonlocal* case, $l \neq 0$. Because the 1D base profile is now uniquely selected [6,9], and furthermore now has a potentially stabilizing surface tension, there is no reason, *a priori,* to expect any instability seen in the local case to persist. And just as a small gradient term strongly modifies the 1D base state (selection for any $l > 0$ but not at $l = 0$), one might expect an equally dramatic modification of the results of any 2D stability calculation.

We linearized the model Eqs. (1)–(3) for small perturbations (lower case) about the (upper case) base profile, $\tilde{\mathbf{\Phi}}(x, y, z, t) = \mathbf{\Phi}(y) + \boldsymbol{\varphi}_{\mathbf{q}}(y)\exp(\omega_{\mathbf{q}} t + iq_x x + iq_z z)$. The vector $\mathbf{\Phi}$ comprises all components $\mathbf{\Phi} = (\Sigma_{\alpha\beta}, V_\alpha)$, the pressure being eliminated by incompressibility. This linearization results in an eigenvalue equation with an operator $\mathcal{L}$ acting linearly on the perturbation $\boldsymbol{\varphi}_{\mathbf{q}}(y)$:

$$\omega_{\mathbf{q}} \boldsymbol{\varphi}_{\mathbf{q}}(y) = \mathcal{L}(\mathbf{\Phi}(y), \mathbf{q}, \partial_y, \partial_y^2, \ldots)\boldsymbol{\varphi}_{\mathbf{q}}(y). \qquad (4)$$

For numerical study, we discretized this equation on a staggered mesh. The 1D base profile $\mathbf{\Phi}(y)$ was read in from the calculation described above. For narrow interfaces, its uniform mesh had too many nodes for use in the numerical eigenvalue problem, so we adapted it to focus attention near the interface. We then calculated the eigenmodes of this discretized problem.

The results, discussed below, were checked: (i) for convergence with respect to mesh structure; (ii) that for a homogeneous base state on the underlying constitutive curve our results match those of Ref. [18]; (iii) that for $a = 1$, $l = 0$ (the local Oldroyd B model), we recover Fig. 3 of Ref. [19]; (iv) that linearization about a semievolved (nonsteady) banded state using the *analytically* derived Eq. (4) gives the same results in the limit $q_x = 0$, $q_z \to 0$ as a direct *numerical* linearization performed in the 1D base state evolver; (v) for robustness with respect to first evolving the base state on either a uniform or adapted grid, using either a semi-implicit or an explicit algorithm; (vi) that two methods of eliminating the pressure (the Oseen tensor and the curl operator) agree.

For any base profile $\mathbf{\Phi}(y)$ and wave vector $\mathbf{q}$, the number of eigenmodes is equal to the number of order parameters summed over all mesh points. We consider only the eigenvalue $\omega_{\max}(\mathbf{q})$ with the largest real part, $\mathrm{Re}\omega_{\max}(\mathbf{q})$. In particular, we ask if this mode is stable, $\mathrm{Re}\omega_{\max} < 0$, or unstable, $\mathrm{Re}\omega_{\max} > 0$. We take $a = 0.3$ and a low solvent viscosity $\eta = 0.05 \ll G\tau \equiv 1$ consistent with experiment, but have checked for robustness to variations in these quantities.

The dispersion relation $\mathrm{Re}\omega_{\max}(q_x, q_z = 0)$ for fluctuations with a wave vector in the direction of the unperturbed flow is shown in Fig. 3 for $\bar{\dot\gamma} = 2.0$. At any q_x, $\mathrm{Re}\omega_{\max}$ increases with decreasing l, and for small enough l [but still larger than the $l = O(100\ \mathrm{nm})$ expected physically] the dispersion relation is positive over a range of wave vectors, rendering the 1D profile unstable. This applies to shear rates right across the banding regime, Fig. 4.

In the limit $l \to 0$, $q_x \to 0$, the corresponding eigenfunction $\{\partial_y v_x, v_y = 0, \sigma_{\alpha\beta}(y)\}$ tends to the spatial derivative of the base state, $\partial_y\{\partial_y V_x, V_y = 0, \Sigma_{\alpha\beta}\}$, representing a simple displacement of the interface in the flow-gradient

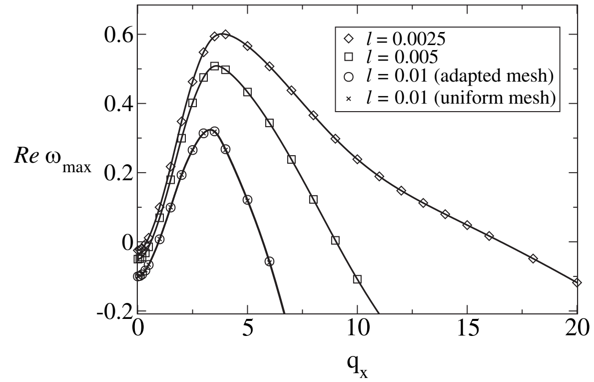

FIG. 3. Real part of the eigenvalue of the most unstable mode. $a = 0.3$, $\eta = 0.05$, $\bar{\dot{\gamma}} = 2.0$, Reynolds number $\rho/\eta = 0$. The data for $l = 0.01$ correspond to the base profile in Fig. 2. Symbols: data. Solid lines: cubic splines.

direction, with small bulk corrections to maintain $\bar{\dot{\gamma}} =$ const. For $q_x > 0$, this displacement is modulated by a wave of wave vector $q_x\hat{\mathbf{x}}$ with an eigenvalue $\omega_{\max}(q_x) = \omega_0 + iq_x\omega_1 + q_x^2\omega_2$ with $\omega_2 > 0$, signifying instability. A natural question is whether this instability resembles that described by McLeish in a local model [12]. As noted above, it is not obvious, *a priori,* that this should be true. Indeed, a detailed analysis is more complicated in this case, and deferred to a future paper. However, the numerical results of Fig. 5 are qualitatively consistent with Ref. [12], as follows. A wavelike interfacial displacement with extrema at $q_x x/2\pi = 0.0, 0.5, 1.0$ causes an interfacial tilt near $q_x x/2\pi = 0.25, 0.75$, exposing the normal stress jump $\Delta\Sigma_{xx}$ across the interface (Fig. 2). This triggers a horizontal perturbation to the flow field $\mathrm{Im}v_x$ in these regions, which recirculates, giving an $O(q_x^2)$ vertical velocity $\mathrm{Re}v_y$ at $q_x x/2\pi = 0.0, 0.5, 1.0$. This enhances the original displacement, causing instability. Stability is restored for higher q_x (Fig. 3), a feature absent in the local case.

The eigenvalue $\mathrm{Re}\omega_{\max}(\mathbf{q})$ over the (q_x, q_z) plane is shown in Fig. 6. Modes with a wave vector along the q_x axis are much more prone to instability than those along the q_z axis. Nonetheless, for smaller values of l (not shown), modes along the line $q_x = 0$ can go unstable as well.

We note finally an important bound on the validity of our calculation. The expansion used to obtain Eq. (4) is valid for perturbations that are small at any point in space: for

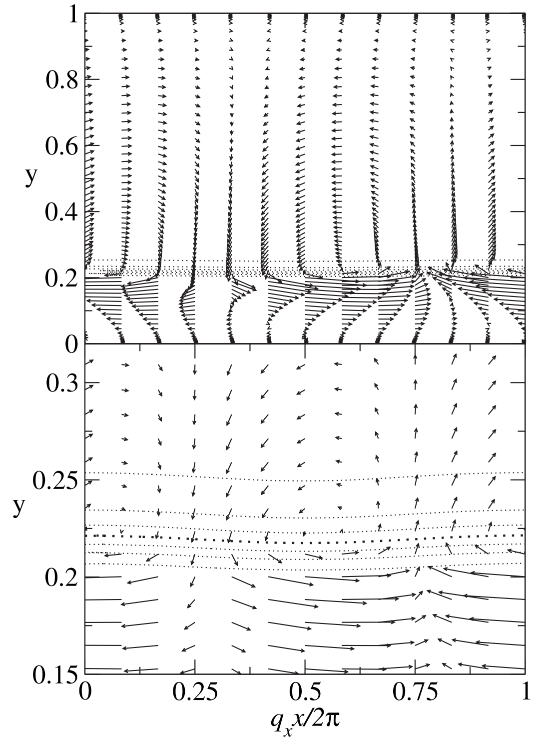

FIG. 5. Perturbation to flow field $s_1\mathrm{Re}\mathbf{v}(y)e^{iq_x x}$ (arrows), and contour lines of perturbed normal stress $\tilde{\Sigma}_{xx}(x, y) = \Sigma_{xx}(y) + s_2\mathrm{Re}\sigma_{xx}(y)e^{iq_x x}$ (dotted lines), corresponding to the eigenvalue of Fig. 3 with $l = 0.01$, $q_x = 2.0$. Contours downwards: 0.45, 0.60, 0.75, 0.90, 1.05, 1.20, 1.35 (middle value shown thicker). Arbitrary scale factors $s_1 = 1.5$ and $s_2 = 0.3$.

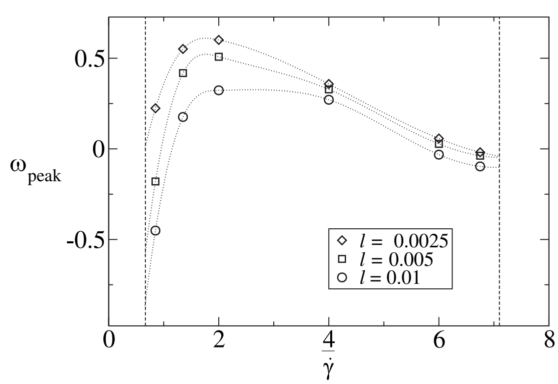

FIG. 4. Peak of the dispersion relation, i.e., $\mathrm{Re}\omega_{\max}$ at $d\mathrm{Re}\omega_{\max}/dq_x = 0$. Parameters as for Fig. 3. Limits of the banding regime shown by vertical lines. Symbols: data. Dotted lines: cubic splines, as a guide to the eye.

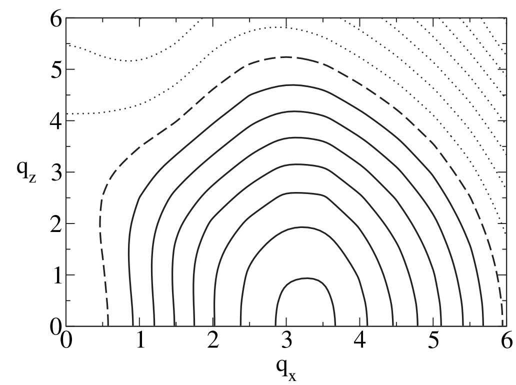

FIG. 6. Real part of the most unstable eigenvalue. $a = 0.3$, $\eta = 0.05$, $\bar{\dot{\gamma}} = 2.0$, Reynolds number $\rho/\eta = 0.01$ (negligible), $l = 0.01$. Contours are $-0.45, -0.40, \ldots$ (dotted line), 0.00 (dashed line), and $\ldots 0.25, 0.30$ (solid line).

example, for the stress components $\sigma_{\alpha\beta} \ll 1$. Displacement of the interface by a distance Δ gives $\sigma_{\alpha\beta} = \Delta d\Sigma_{\alpha\beta}/dy$, which is $O(\Delta/l)$, because the interfacial width is $O(l)$. We are thus restricted to displacements, $\Delta \ll l$. In future work, we consider $\Delta \gg l$.

We comment briefly on the stability of a sheared interface between phases of a binary fluid in "model H" [20]. Although this was studied in Ref. [21], that work used a single equation for the position of the interface, therefore neglecting changes in the interface's profile. Nonetheless, we too found the interface to be stable. This supports the idea that normal stresses (absent in model H) cause the instability described above. We also note the fundamental difference between this instability, which occurs due to viscoelastic effects even in the inertialess limit, and others such as the Kelvin Helmholtz instability [22], seen in nonviscoelastic fluids due to inertial effects.

To conclude, we have found 1D planar shear banded flow to be linearly unstable to fluctuations with a wave vector in the plane of the banding interface, within the DJS model. This applies to shear rates right across the stress plateau, suggesting that the instability is ubiquitous and that the existing theoretical picture of two stable shear bands separated by a steady interface needs more thought. Indeed, our finding is consistent with accumulating evidence for erratic fluctuations [10] and band breakup [23]. Future work will study the fate of the interface beyond the validity of this linear study. One possibility is that the instability is self-limiting beyond some amplitude set by l (e.g., $l^{1/2}$). This would be consistent with a narrowly localized but still unsteady interface, which might be interpreted as steady in experiments that did not have high spatial resolution (perhaps reconciling early reports of apparently steady interfaces with recent work revealing fluctuations).

By contrast, if the instability were not self-limiting, and yet ubiquitous in existing banding models, one would need a new theoretical picture of (reasonably) steady shear bands that could still accommodate the normal stress jump across the interface. Other open questions include the status of the instability in curved Couette geometry, and the relative importance of instabilities at nonzero $\mathbf{q}$ (as studied here) to those found at zero $\mathbf{q}$ in recent models of spatiotemporal rheochaos [24].

The author thanks Paul Callaghan, Mike Cates, Tanniemola Liverpool, Tom McLeish, Peter Olmsted, and Helen Wilson for useful discussions and feedback, and the EPSRC GR/S29560/01 for funding.

*Present address: School of Mathematics, University of Manchester, Booth St. East, Manchester M13 9EP, U.K.
Electronic address: suzanne.fielding@manchester.ac.uk

[1] M. M. Britton and P. T. Callaghan, Phys. Rev. Lett. **78**, 4930 (1997).

[2] O. Diat, D. Roux, and F. Nallet, J. Phys. II (France) **3**, 1427 (1993).

[3] L. Hilliou and D. Vlassopoulos, Ind. Eng. Chem. Res. **41**, 6246 (2002).

[4] J. S. Raynaud, P. Moucheront, J. C. Baudez, F. Bertrand, J. P. Guilbaud, and P. Coussot, J. Rheol. (N.Y.) **46**, 709 (2002).

[5] M. Doi and S. F. Edwards, *The Theory of Polymer Dynamics* (Clarendon, Oxford, 1989); M. E. Cates, J. Phys. Chem. **94**, 371 (1990); M. Doi, J. Polym. Sci., Polym. Phys. Ed. **19**, 229 (1981); P. D. Olmsted and C.-Y. D. Lu, Phys. Rev. E **60**, 4397 (1999).

[6] C.-Y. D. Lu, P. D. Olmsted, and R. C. Ball, Phys. Rev. Lett. **84**, 642 (2000).

[7] N. A. Spenley, M. E. Cates, and T. C. B. McLeish, Phys. Rev. Lett. **71**, 939 (1993); P. D. Olmsted and P. M. Goldbart, Phys. Rev. A **41**, 4578 (1990).

[8] M. Johnson and D. Segalman, J. Non-Newtonian Fluid Mech. **2**, 255 (1977).

[9] P. D. Olmsted, O. Radulescu, and C.-Y. D. Lu, J. Rheol. (N.Y.) **44**, 257 (2000).

[10] A. S. Wunenburger, A. Colin, J. Leng, A. Arneodo, and D. Roux, Phys. Rev. Lett. **86**, 1374 (2001); R. Bandyopadhyay, G. Basappa, and A. K. Sood, Phys. Rev. Lett. **84**, 2022 (2000); W. M. Holmes, M. R. Lopez-Gonzalez, and P. T. Callaghan, Europhys. Lett. **64**, 274 (2003); Y. T. Hu, P. Boltenhagen, and D. J. Pine, J. Rheol. (N.Y.) **42**, 1185 (1998); P. Fischer, E. K. Wheeler, and G. G. Fuller, Rheol. Acta **41**, 35 (2002).

[11] S. Manneville, J. B. Salmon, and A. Colin, Eur. Phys. J. E **13**, 197 (2004); J. B. Salmon, L. Becu, S. Manneville, and A. Colin, Eur. Phys. J. E **10**, 209 (2003); M. R. López-González, W. M. Holmes, P. T. Callaghan, and P. J. Photinos, Phys. Rev. Lett. **93**, 268302 (2004).

[12] T. C. B. McLeish, J. Polym. Sci., Part B: Polym. Phys. **25**, 2253 (1987).

[13] A. W. El-Kareh and L. G. Leal, J. Non-Newtonian Fluid Mech. **33**, 257 (1989); J. L. Goveas and G. H. Fredrickson, Eur. Phys. J. B **2**, 79 (1998).

[14] J. Yerushalmi, S. Katz, and R. Shinnar, Chem. Eng. Sci. **25**, 1891 (1970).

[15] W. H. Press, S. A. Teukolsky, W. T. Vetterling, and B. P. Flannery, *Numerical Recipes in C* (Cambridge University Press, Cambridge, 1992).

[16] Y. Y. Renardy, Theor. Comput. Fluid Dyn. **7**, 463 (1995).

[17] E. J. Hinch, O. J. Harris, and J. M. Rallison, J. Non-Newtonian Fluid Mech. **43**, 311 (1992).

[18] S. M. Fielding and P. D. Olmsted, Phys. Rev. E **68**, 036313 (2003).

[19] H. J. Wilson, M. Renardy, and Y. Renardy, J. Non-Newtonian Fluid Mech. **80**, 251 (1999).

[20] P. C. Hohenberg and B. I. Halperin, Rev. Mod. Phys. **49**, 435 (1977).

[21] A. J. Bray, A. Cavagna, and R. D. M. Travasso, Phys. Rev. E **65**, 016104 (2002).

[22] T. E. Faber, *Fluid Dynamics for Physicists* (Cambridge University Press, Cambridge, 1995).

[23] S. Lerouge, Ph.D. thesis, University of Metz, 2000.

[24] S. M. Fielding and P. D. Olmsted, Phys. Rev. Lett. **92**, 084502 (2004); A. Aradian and M. E. Cates, Europhys. Lett. **70**, 397 (2005).